# Chapter 6

# Underwater granular flows

## 6.1 Introduction

Avalanches, landslides, and debris flows are geophysical hazards, which involve rapid mass movement of granular solids, water, and air as a single phase system. Globally, landslides cause billions of pounds in damage, and thousands of deaths and injuries each year. Hence, it is important to understand the triggering mechanism and the flow evolution. The momentum transfer between the discrete and continuous phases significantly affects the dynamics of the flow as a whole (Topin et al., 2012). Although certain macroscopic models are able to capture simple mechanical behaviours (Peker and Helvacı, 2007), the complex physical mechanisms occurring at the grain scale, such as hydrodynamic instabilities, formation of clusters, collapse, and transport, (Topin et al., 2011) have largely been ignored. In particular, when the solid phase reaches a high volume fraction, the strong heterogeneity arising from the contact forces between the grains, and the hydrodynamic forces, are difficult to integrate into the homogenization process involving global averages.

In order to describe the mechanism of immersed granular flows, it is important to consider both the dynamics of the solid phase and the role of the ambient fluid (Denlinger and Iverson, 2001). The dynamics of the solid phase alone is insufficient to describe the mechanism of granular flow in a fluid. It is important to consider the effect of hydrodynamic forces that reduce the weight of the solids inducing a transition from dense-compacted to dense-suspended flows, and the drag interactions which counteract the movement of the solids (Meruane et al., 2010). Transient regimes characterized by change in the solid fraction, dilation at the onset of flow and development of excess pore pressure, result in altering the balance between the stress carried by the fluid and that carried by the grains, thereby changing the overall behaviour of the flow.

The presence of a fluid phase in a granular medium has profound effects on its mechanical behaviour. In dry granular media the rheology is governed by grain inertia and static stresses sustained by the contact network depending on the shear-rate and confining pressure, respectively (Midi, 2004). As the fluid inertia and viscosity come into play, complications arise as a result of contradictory effects. On one hand, the fluid may delay the onset of granular flow or prevent the dispersion of the grains by developing negative pore pressures (Pailha et al., 2008; Topin et al., 2011). On the other hand, the fluid lubricates the contacts between grains, enhancing in this way the granular flow, and it has a retarding effect at the same time by inducing drag forces on the grains. The objective of the present study is to understand the differences in the mechanism of flow initiation and kinematics between dry and submerged granular flow. In the present study, 2D Lattice-Boltzmann and Discrete Element Method is used to model the fluid-soil interactions in underwater granular flows.

## 6.2 Granular collapse in fluid

The collapse of a granular column, which mimics the collapse of a cliff, has been extensively studied in the case of dry granular material, when the interstitial fluid plays no role (see **??**). The problem of the granular collapse in a liquid,which is of importance for submarine landslides, has to our knowledge attracted less attention (Rondon et al., 2011). Thompson and Hupper (2007) observed that the presence of liquid dramatically changes the way a granular column collapses compared to the dry case. The destabilization of a granular pile strongly depends on the initial volume fraction of the packing. For dense packings the granular flow is localized at the free surface of the pile, whereas for loose packings the destabilization occurs in the bulk of the material and has a parabolic profile (Bonnet et al., 2010; Iverson, 2000; Topin et al., 2011). In the present study, the collapse of a granular column in fluid is studied using 2D LBM - DEM and the flow kinematics is compared with dry granular collapse. The role of permeability and initial volume fraction on the run-out behaviour is also investigated.

### 6.2.1 LBM-DEM Coupling

Lattice Boltzmann approach can accommodate large grain sizes and the interaction between the fluid and the moving grains can be modelled through a relatively simple fluid – grain interface treatment. Further, employing the Discrete Element Method (DEM) to account for the grain – grain interaction naturally leads to a combined LB – DEM procedure (Mansouri et al., 2009).

In this study, a 2D poly-disperse system ($d_{max}/d_{min} = 1.8$) of circular discs in fluid is used to simulate the behaviour of granular collapse in fluid (see Figure 6.1). A cumulative $\beta$ distribution

is adopted to generate grains with $d_{max}$ and $d_{min}$ as 1.25 mm and 2.2 mm, respectively. The soil column is modelled using $\approx 2000$ discs of density $2650\,\mathrm{kg\,m^{-3}}$ and a contact friction angle of 26°. A linear-elastic contact model is used in DEM simulations. The collapse of the column was simulated inside a fluid with a density of $1000\,\mathrm{kg\,m^{-3}}$ and a kinematic viscosity of $1 \times 10^{-6}\,\mathrm{m^2\,s^{-1}}$. The gravity angle $\theta$ is set to zero to simulate collapse onto a horizontal surface. The choice of a 2D geometry has the advantage of cheaper computational effort than a 3D case, making it feasible to simulate very large systems.

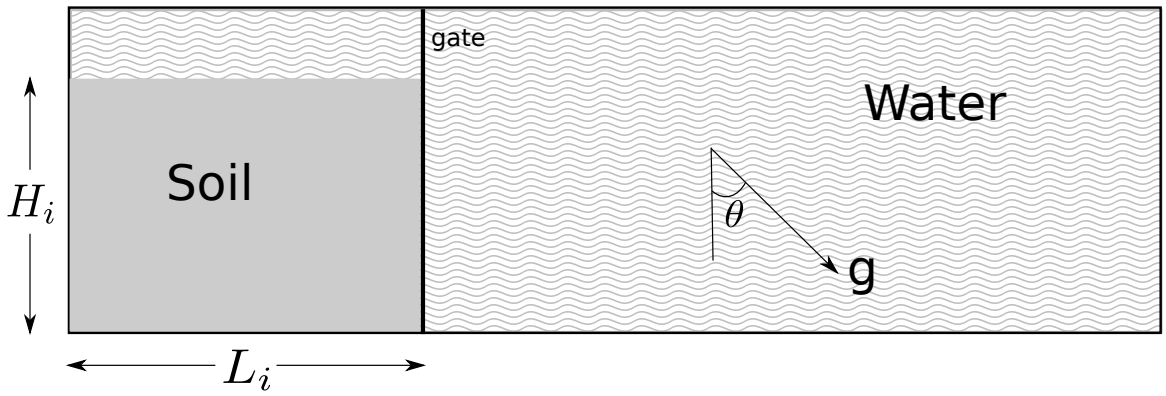


Figure 6.1 Underwater granular collapse set-up.

The Eulerian nature of the LBM formulation, together with the common explicit time step scheme of both LBM and DEM makes this coupling strategy an efficient numerical procedure for the simulation of grain – fluid systems. The critical time step for DEM is computed based on the local contact natural frequency and damping ratio. A sub-cycling time integration is adopted in DEM (see **??**). A fluid flow (LBM) time step, $\Delta t = 2.0E^{-}5s$ is determined based on the viscosity and relaxation parameter $\tau = 0.506$. An integer ratio $n_s$, between the fluid flow time step $\Delta t$ and DEM time step $\Delta t_D$ is determined as 15, i.e., every LBM iteration involves a sub-cycle of 15 DEM iterations.

In order to capture realistic physical behaviour of the fluid – grain system, it is essential to model the boundary condition between the fluid and the grain as a non-slip boundary condition, i.e. the fluid near the grain should have similar velocity as the grain boundary. The solid grains inside the fluid are represented by lattice nodes. The discrete nature of lattice, results in a stepwise representation of the surfaces (see figure 6.2), which are circular, hence sufficiently small lattice spacing $h$ is required. The smallest DEM grain in the system controls the length of the lattice spacing. In the present study, a very fine discretisation of $d_{min}/h = 10$ is adopted, i.e., the smallest grain with a diameter $d_min$ in the system is discretised into 100 lattice nodes ($10h \times 10h$). This represents a very accurate representation of the interaction between the solid and the fluid nodes.

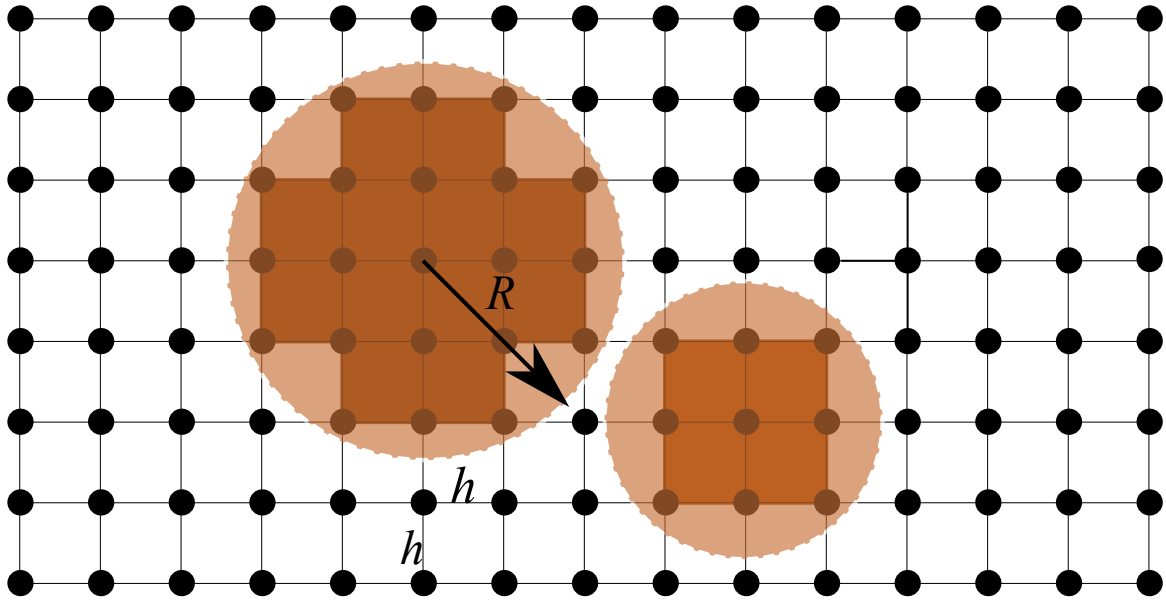


Figure 6.2 Discretisation of solid grains in LBM grid. Shows the step-wise representation of circular disks in the lattice.

### 6.2.2 Permeability

In DEM, the grain – grain interaction is described based on the contact interactions. In a 3D granular assembly, the pore spaces between grains are interconnected, whereas in a 2-D assembly, the grains are in contact with each other and this results in a non-interconnected pore-fluid space. Which means that the pore-fluid enclosed between the grains cannot flow to neighbouring pore-space. This results in a unnatural no flow condition in a 2-D case (see figure 6.3). In order to overcome this difficulty, a reduction in radius is assumed only during LBM computations (fluid and fluid – solid interaction). The reduced radius of the soil grain, i.e., the *hydrodynamic radius* 'r', allows for interconnected pore space through which the pore-fluid can flow similar to 3D behaviour. The reduction in radius is assumed only during LBM computations, hence this technique has no effect on the grain – grain interactions computed using DEM.

Realistically, the hydrodynamic radius can be varied from $r = 0.7R$ to $0.95R$, where 'R' is the grain radius. Different permeability can be obtained, for any given initial packing, by varying the hydrodynamic radius of the grains, without changing the actual granular packing. Hence, the hydrodynamic radius represents the permeability of the granular assembly. In another sense, the hydrodynamic radius can be assumed to represent the irregularities on the granular surface. Reducing the hydrodynamic radius represents wider channel and more flow between the grains.

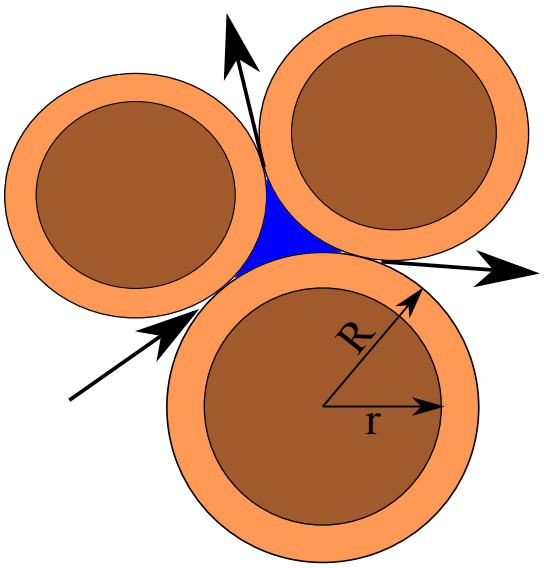


Figure 6.3 Schematic representation of the hydrodynamic radius in LBM-DEM computation

In order to understand the relation between the hydrodynamic radius and the permeability of the granular assembly, horizontal permeability tests are performed by varying the hydrodynamic radius as 0.7R, 0.75R, 0.8R, 0.85R, 0.9 and 0.95R. A square sample of 50 mm $\times$ 50 mm is used to determine the transverse permeability. Dirichlet boundary condition (discussed in **??**), i.e., pressure/density constrain is applied along the left and the right boundaries. The density on the left boundary is increased in small increments ($10^{-4}\Delta P$), which a constant density is maintained on the right boundary. This results in a pressure gradient causing the fluid to flow (see figure 6.4).

The mean velocity of flow (v) is determined and the permeability of the sample (k) is computed as:

$$k = v \cdot \mu \cdot \frac{\Delta x}{\Delta P}, \tag{6.1}$$

where $\mu$ is the dynamic viscosity of the fluid (Pa s), $\Delta x$ is the thickness of the bed of porous medium m, and $\Delta P$ is the applied pressure difference Pa. For a given hydrodynamic radius, the pressure gradient $\Delta P$ is varied to obtain different flow rates. Probing the fluid space showed a Poiseuille flow behaviour between grains. The flow is still within the Darcy's laminar flow regime, which is verified by the linear slope between the pressure gradient and mean flow velocity (see figure 6.5). It can be observed that with increase in the hydrodynamic radius the permeability decreases, i.e., the slope of the mean flow velocity to the pressure gradient decreases. At very low pressure gradient ($\Delta P \leq 0.1$), both 0.9R and 0.95r has a no flow condition. A hydrodynamic radius of $r = 0.95R$ shows almost no flow behaviour, even at higher pressure gradients. A high value of hydrodynamic radius $r > 0.95R$ results in unnatural flow

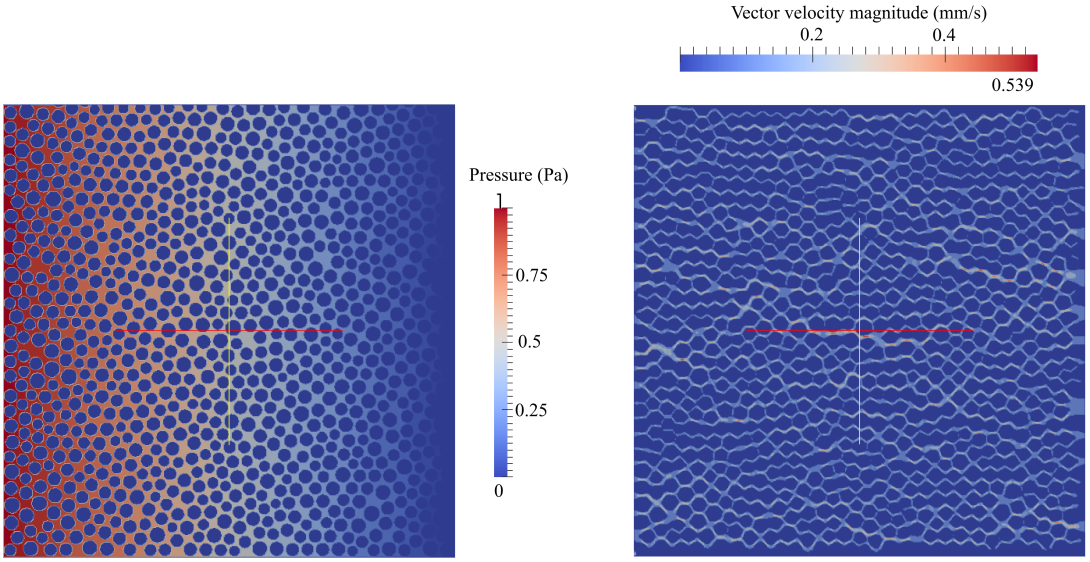


(a) Pressure gradient in the granular assembly (b) Horizontal flow due to pressure gradient

Figure 6.4 Evaluation of the horizontal permeability for a hydrodynamic radius of 0.7R.

behaviour. Hence, hydrodynamic radii in the range of 0.7 to 0.95R are adopted in the present study.

Increase in the hydrodynamic radius from 0.7 to 0.95 reduces the porosity from 0.60 to 0.27. The permeability computed from LB – DEM method is verified by comparing it with the analytical solution. One of the widely used analytical solution for permeability is the Carman – Kozeny equation (CK Model), which is based on the Poiseuille flow through a pipe and is mainly used for 3D, homogeneous, isotropic, granular porous media at moderate porosities. In the present study, a modified Carman – Kozeny equation that takes into account the micro-structure of the fibres and that is valid in a wide range of porosities is adopted (**?**). The normalized permeability is defined as

$$\frac{k}{d^2} = \frac{\varepsilon}{\psi_{CK}(1-\varepsilon)^2}\,. \tag{6.2}$$

In the CK model, the hydraulic diameter $D_h$ , is expressed as a function of measurable quantities: porosity and specific surface area

$$D_h = \frac{4\varepsilon V}{S_v} = \frac{\varepsilon d}{(1-\varepsilon)}\,, \tag{6.3}$$

$$a_v = \frac{\text{grain surface}}{\text{grain volume}} = \frac{S_v}{(1-\varepsilon V)} = \frac{4}{d}\,, \tag{6.4}$$

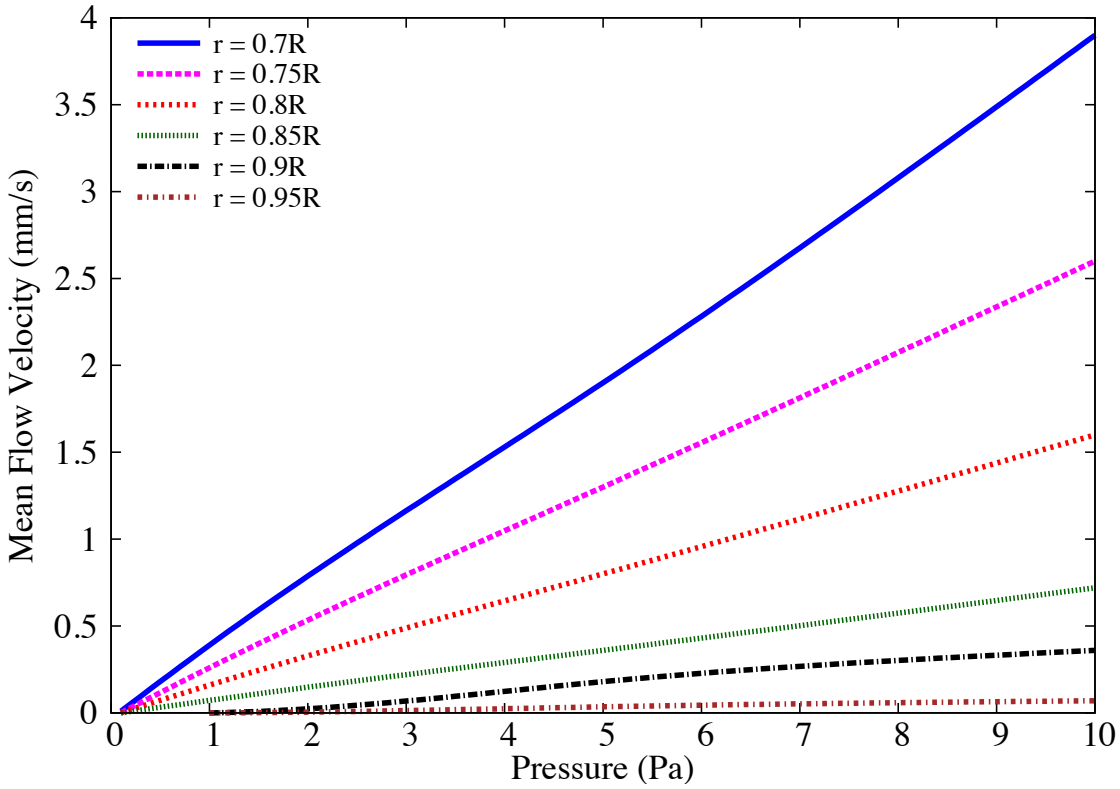


Figure 6.5 Variation of the mean flow velocity with pressure gradient for different hydrodynamic radius.

where $S_v$ is the total wetted surface, and $a_v$ is the specific surface area. The above value of $a_v$ is for circles (cylinders) - for spheres $a_v = 6/d$. $\psi_{CK}$ is the empirically measured CK factor, which represents both the shape factor and the deviation of flow direction from that in a duct. It is approximated for randomly packed beds of spherical grains. The normalized permeability for different porosity obtained by varying the radius from 0.7 to 0.95 is presented in figure 6.6. The normalized permeability is found to match the qualitative trend of the Carman-Kozeny equations. The LB – DEM permeability curve lies between the permeability curves for spherical and cylindrical grain arrangements implying a better approximation of permeability in 2D granular assembly by reducing the radius during LBM computations.

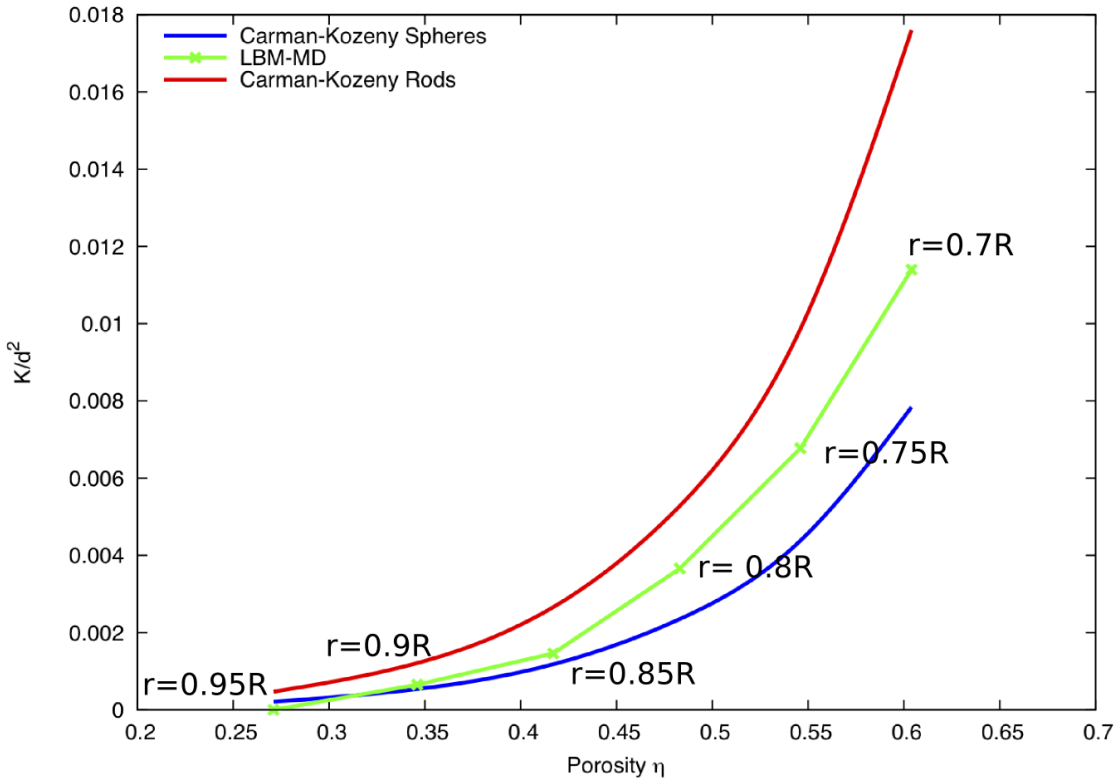


Figure 6.6 Relation between permeability and porosity for different hydrodynamic radius and comparison with the analytical solution.

### 6.2.3 Collapse in fluid: Flow evolution

A granular column of aspect ratio ‘a’ of 0.8 was used. A hydrodynamic radius r = 0.9R was adopted during the LBM computations. Dry analyses were also performed to study the effect of hydrodynamic forces on the run-out distance.x

## 6.3 Submarine granular flows down incline plane

The flow of dense granular material is a common phenomenon in engineering predictions, such as avalanches, landslides, and debris-flow modelling. Despite the huge amount of research that has gone into describing the behaviour of granular flows, a constitutive equation that describes the overall behaviour of a flowing granular material is still lacking. The initiation and propagation of submarine granular flows depend mainly on the slope, density, and quantity of the material destabilised. Although certain macroscopic models are able to capture the simple mechanical behaviours, the complex physical mechanisms that occur at the grain scale, such as thydrodynamic instabilities, the formation of clusters, collapse, and transport, have largely been ignored (Topin et al., 2011). The momentum transfer between the discrete and the continuous phases significantly affects the dynamics of the flow (Peker and Helvacı, 2007). Grain-scale description of the granular material enriches the macro-scale variables, which poorly account for the local rheology of the materials. In order to describe the mechanism of saturated and/or immersed granular flows, it is important to consider both the dynamics of the solid phase and the role of the ambient fluid (Denlinger and Iverson, 2001). In particular, when the solid phase reaches a high volume fraction, it is important to consider the strong heterogeneity arising from the contact forces between the grains, the drag interactions which counteract the movement of the grains, and the hydrodynamic forces that reduce the weight of the solids inducing a transition from dense compacted to a dense suspended flow (Meruane et al., 2010). The case of the collapse in presence of an interstitial fluid has been less studied. In this paper, we study the submarine granular flows in the inclined configuration. We study the effect of permeability, density and slope angle on the run-out evolution.

In this study, a 2D poly-disperse system ($d_{max}/d_{min} = 1.8$) of circular discs in fluid was used to understand the behaviour of granular flows on inclined planes (see **??**). The soil column was modelled using 1000 discs of density 2650 $\mathrm{kg\,m^{-3}}$ and a contact friction angle of 26°. The collapse of the column was simulated inside a fluid with a density of 1000 $\mathrm{kg\,m^{-3}}$ and a kinematic viscosity of $1 \times 10^{-6}\,\mathrm{m^2\,s^{-1}}$. The choice of a 2D geometry has the advantage of cheaper computational effort than a 3D case, making it feasible to simulate very large systems. A granular column of aspect ratio 'a' of 0.8 was used. A hydrodynamic radius r = 0.9R was adopted during the LBM computations. Dry analyses were also performed to study the effect of hydrodynamic forces on the run-out distance.

### 6.3.1 Effect of initial density

The morphology of the granular deposits in fluid is shown to be mainly controlled by the initial volume fraction of the granular mass and not by the aspect ratio of the column (Pailha et al.,

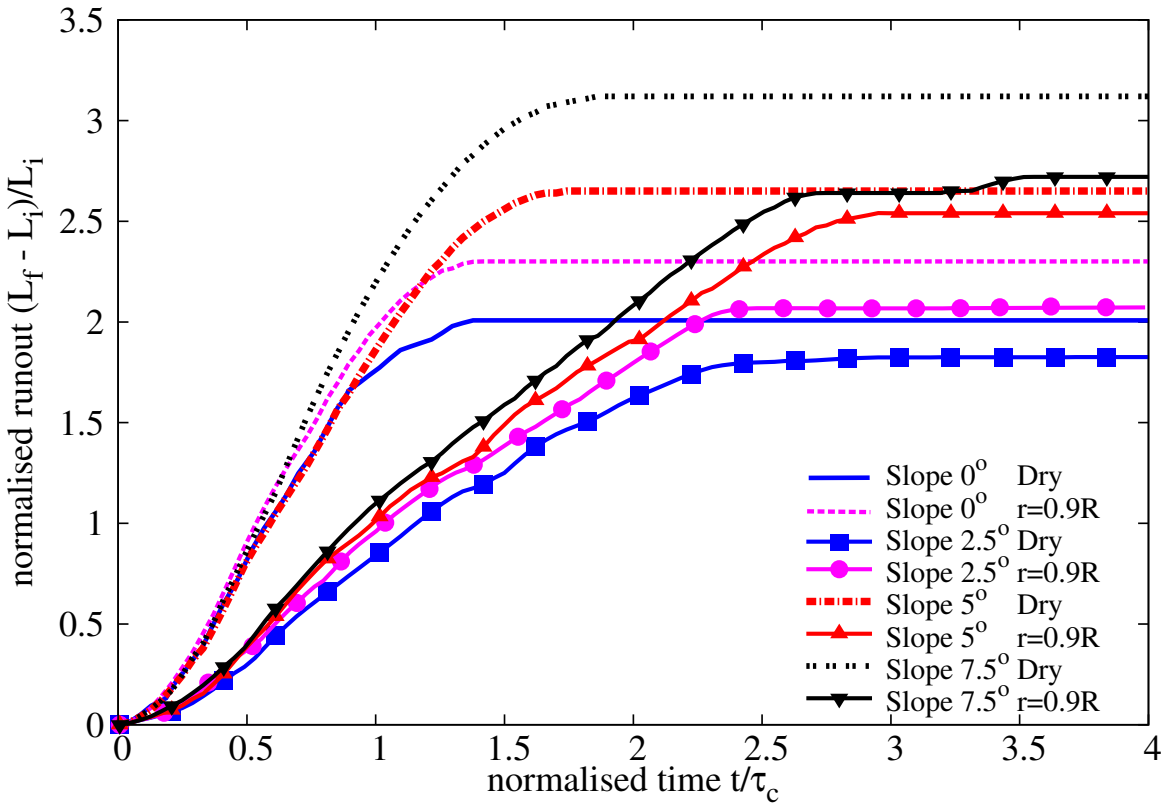


Figure 6.7 Evolution of run-out with time (dense)

2008; Rondon et al., 2011). In order to understand the influence of the initial packing density on the run-out behaviour, a dense sand column (initial packing density, $\Phi = 83\%$) and a loose sand column ($\Phi = 79\%$) were used. The granular columns collapse and flow down slopes of varying inclinations (2.5°, 5° and 7.5°).

The evolution of run-out distances for a dense sand column with time in dry and submerged conditions for varying slope inclinations are presented in figure 6.7. The run-out distance is longer in submerged condition than the dry condition for a flow on a horizontal surface. However, with increase in the slope angle the run-out in the fluid decreases.

Dense granular columns in fluid take a longer time to collapse and flow, due to the development of large negative pore-pressures, as the dense granular material dilates during the initial phase of the flow. The morphology of dense granular flows down slopes of varying inclinations at the critical time ($t = \tau_c = \sqrt{H/g}$, when the flow is fully mobilised) are shown in figure 6.9.

It can be seen that the viscous drag on the dense column tend to predominate over the influence of hydroplaning on the run-out behaviour. This influence can be observed in the smaller peak kinetic energy for granular column in fluid compared to it's dry counterpart (see Figure 6.8). With increase in slope angle, the volume of material that dilates increases.

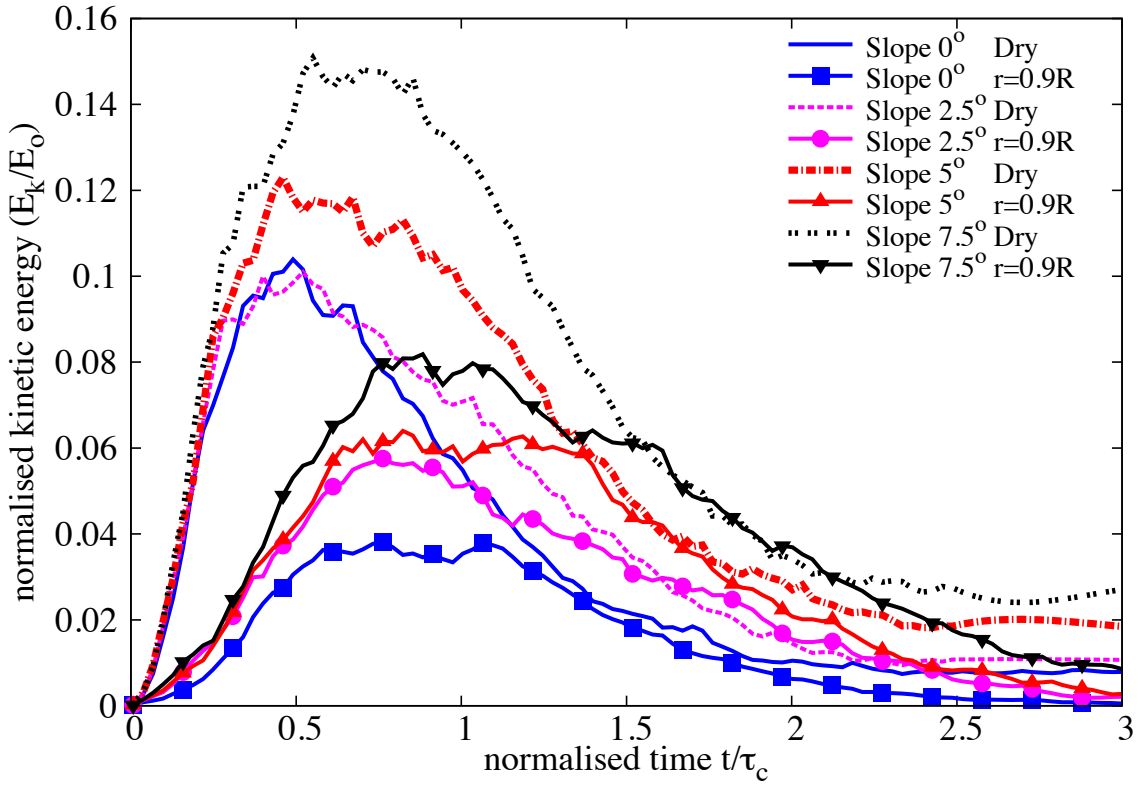


Figure 6.8 Evolution of Kinetic Energy with time (dense case)

This results in large negative pore pressures and more viscous drag on the granular material. Hence, the difference in the run-out between the dry and the submerged condition, for a dense granular assembly, increases with increase in the slope angle.

In contrast to the dense granular columns, the loose granular columns (relative density $I_D = 30\%$) show longer run-out distance in immersed conditions (see Figure 6.10). The run-out distance in fluid increases with increase in the slope angle compared to the dry cases. Loose granular material tends to entrain more water at the base of the flow front, creating a lubricating surface, which causes longer run-out distance (see Figure 6.11). The hydroplaning effect causes an increase in the velocity the loose condition in comparison with the dense condition (see Figure 6.12).

The evolution of packing density (see Figure 6.13) shows that dense and the loose conditions reach similar packing density. This indicates that the dense granular column dilates more and is susceptible to higher viscous drag forces. Where as in the loose condition, a positive pore-pressure is observed at the base of the flow, indicating entrainment of water at the base, i.e. hydroplaning resulting in longer run-out distance.

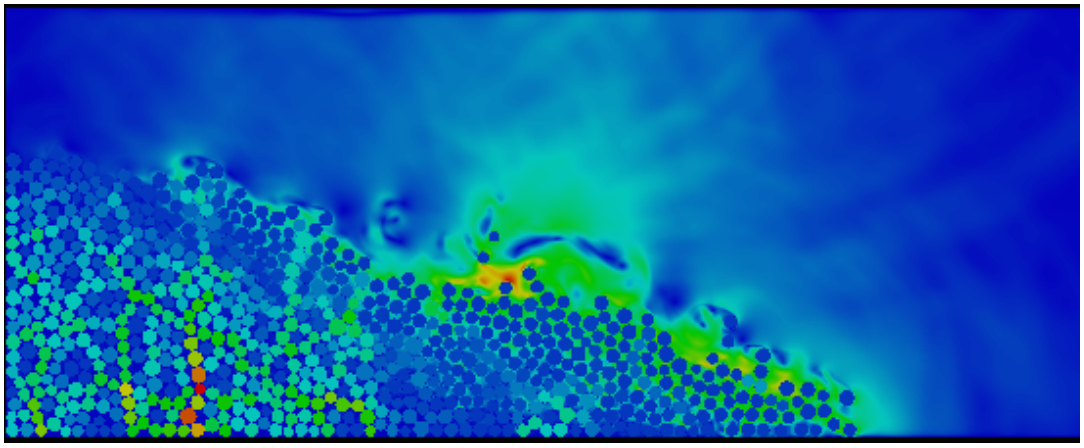

(a) Slope 2.5

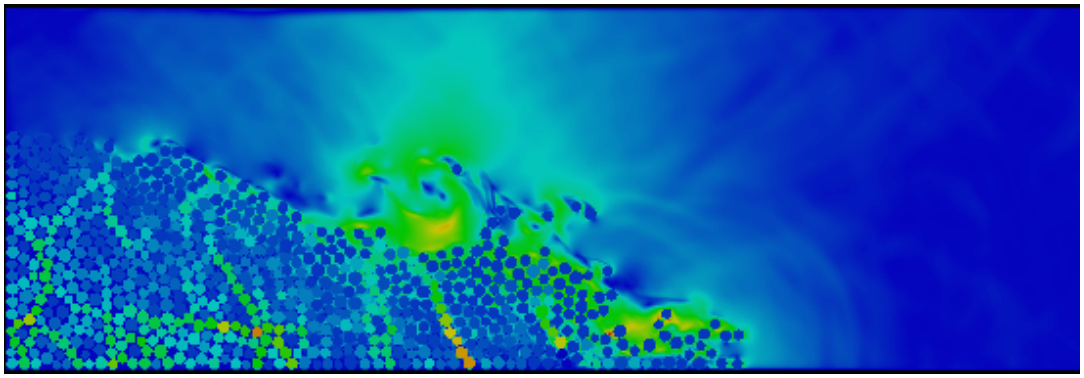

(b) Slope 5.0

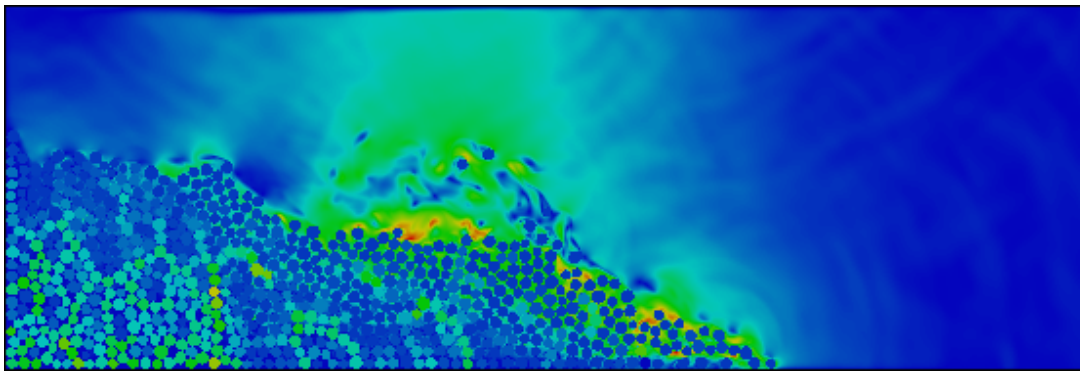

(c) Slope 7.5

Figure 6.9 Flow morphology at critical time for different slope angles (dense)

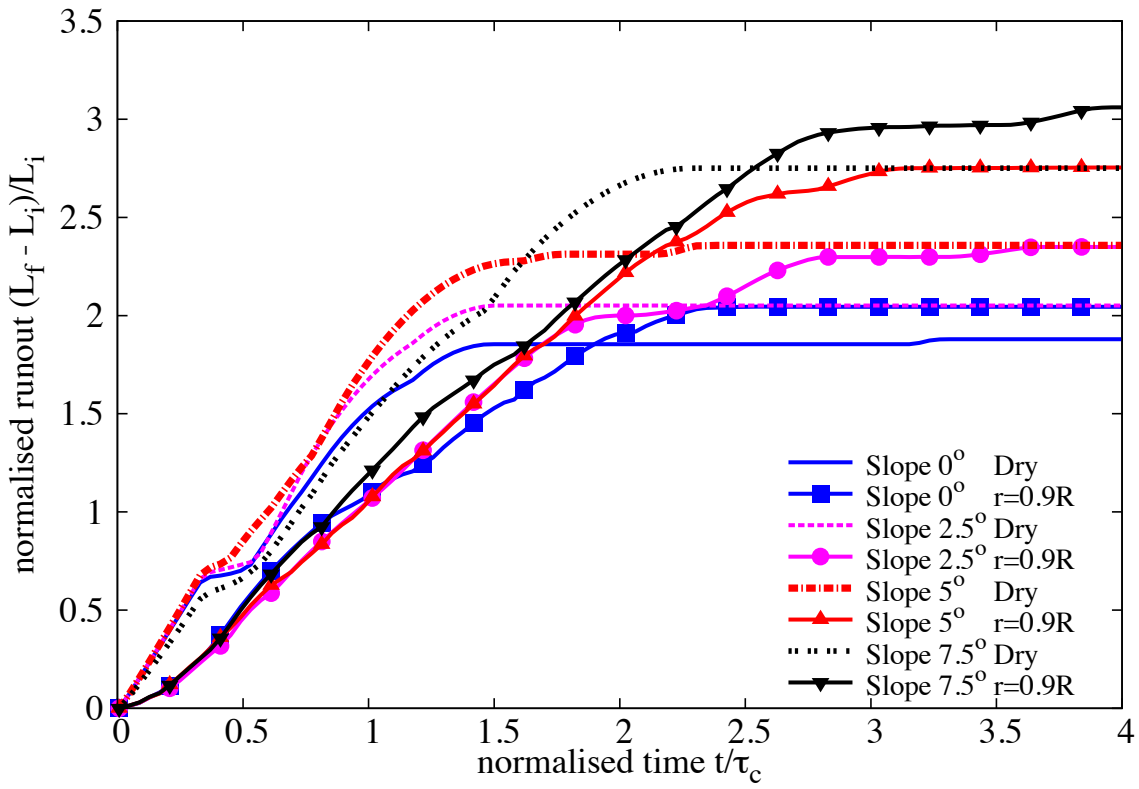


Figure 6.10 Evolution of run-out with time (loose)

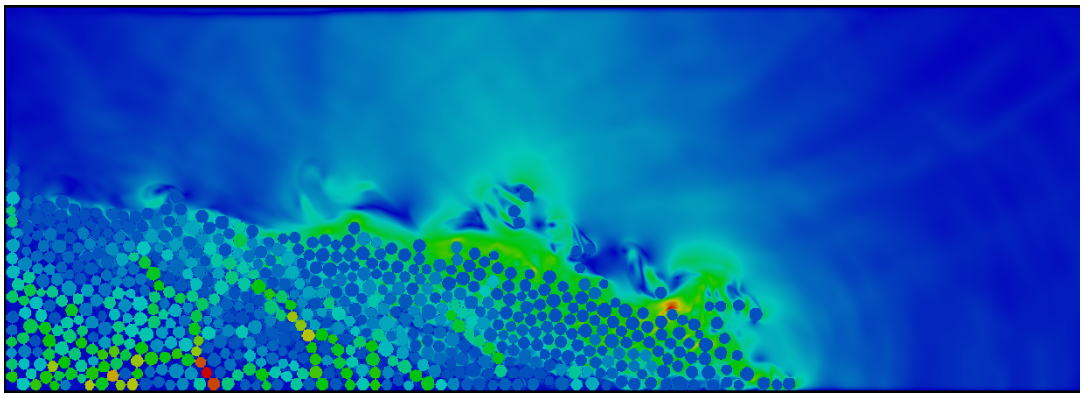

(a) Slope 2.5

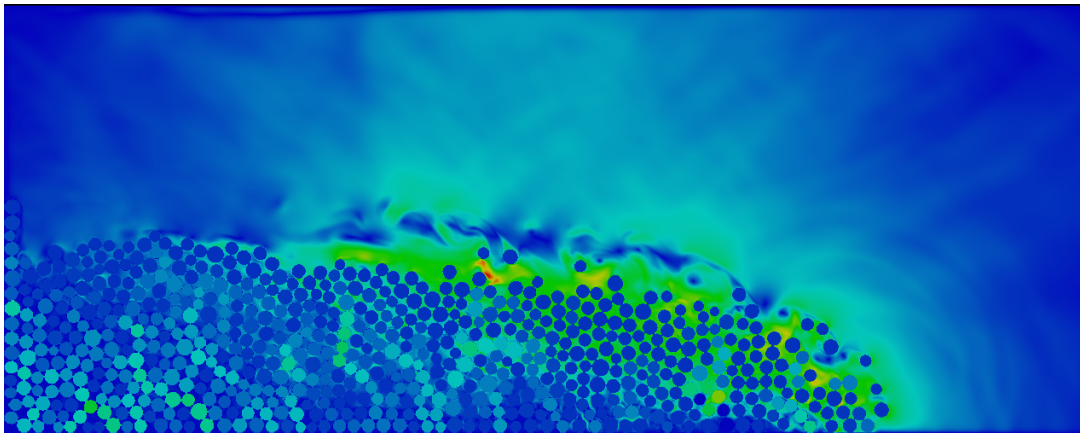

(b) Slope 5.0

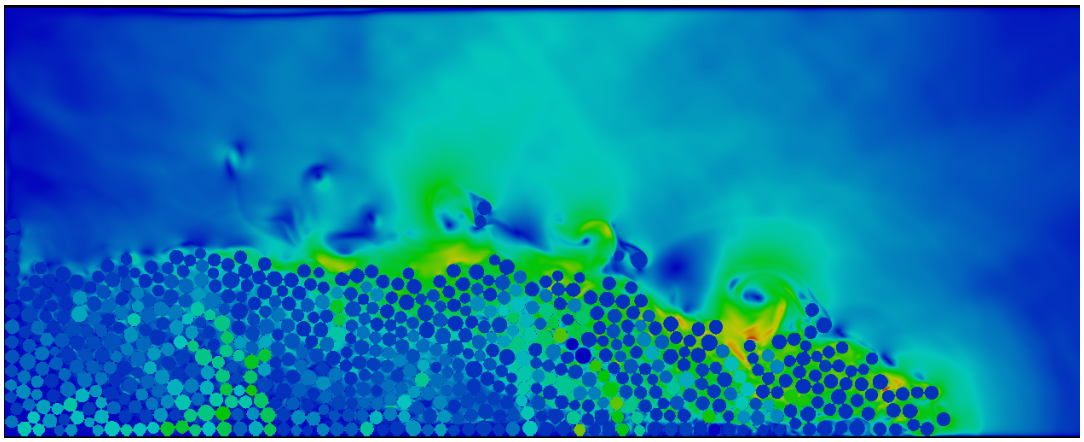

(c) Slope 7.5

Figure 6.11 Flow morphology at critical time for different slope angles (loose)

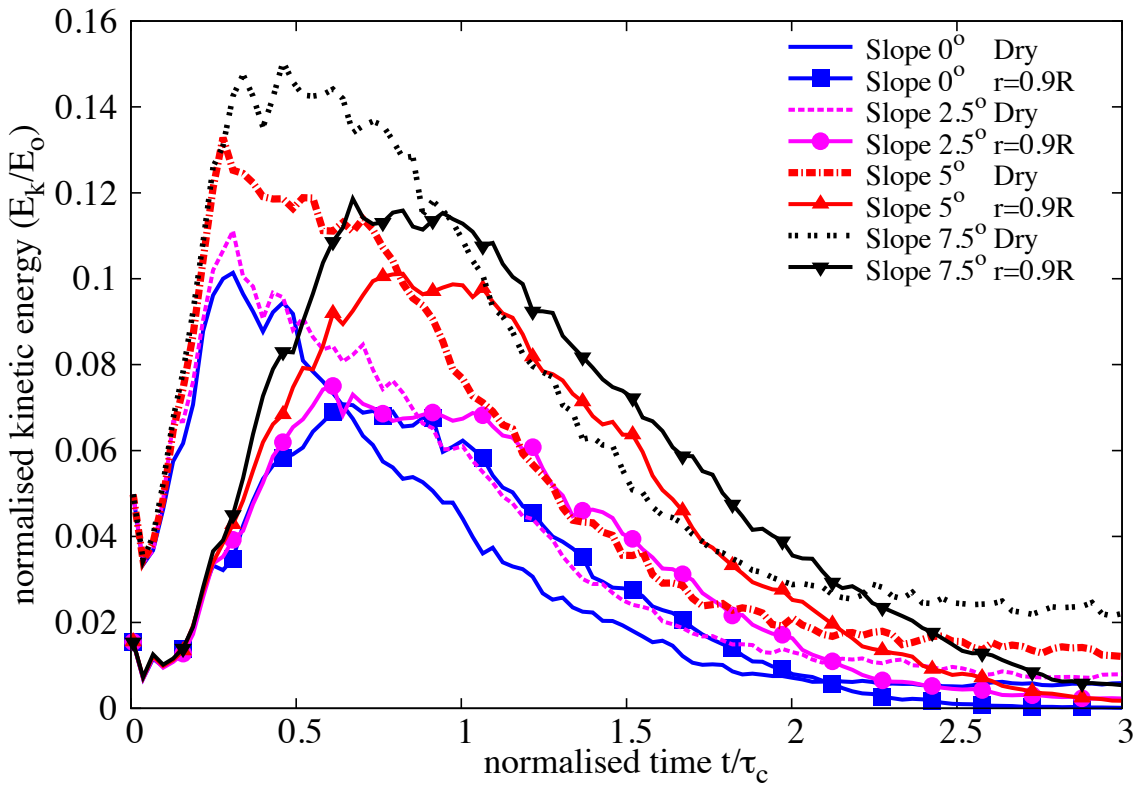


Figure 6.12 Evolution of Kinetic Energy with time (loose)

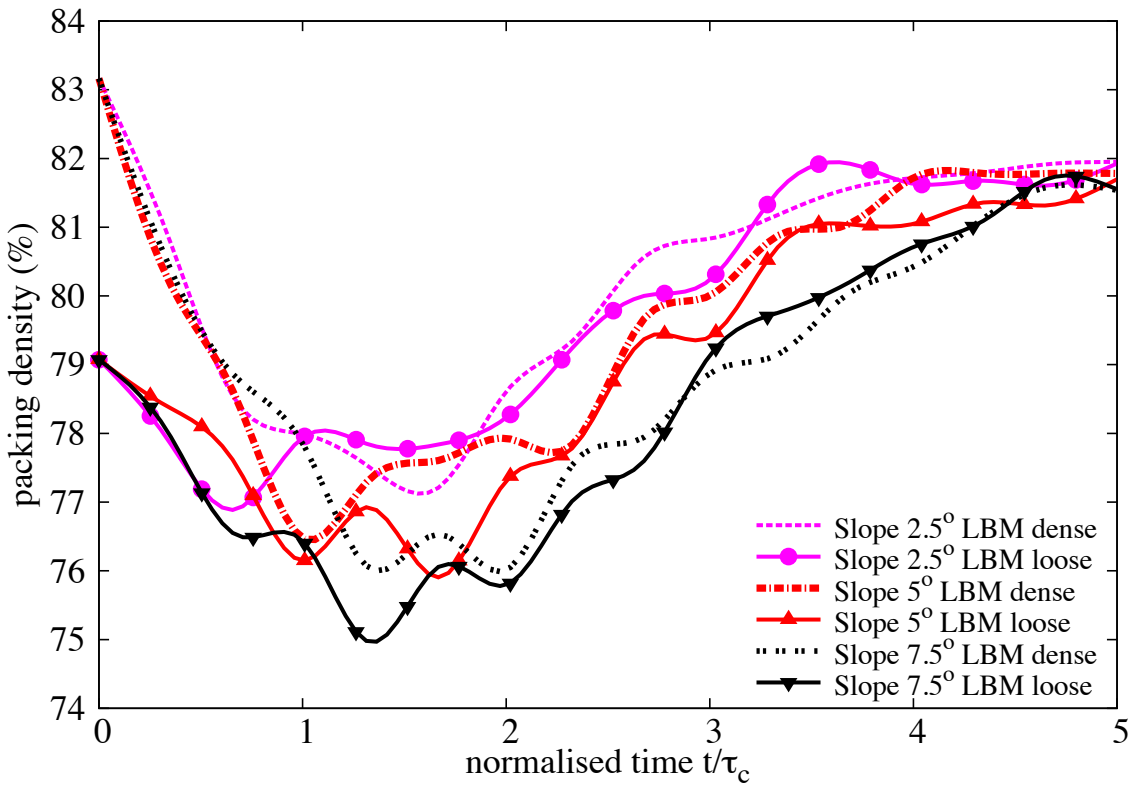


Figure 6.13 Evolution of packing density with time

### 6.3.2 Effect of permeability

In DEM, the grain – grain interaction is described based on the overlap between the grains at the contact surface. In a 3D granular assembly, the pore spaces between grains are interconnected. Whereas in a 2-D assembly, the grains are in contact with each other that result in a non-interconnected pore-fluid space. This causes a no flow condition in a 2-D case. In order to overcome this difficulty, a reduction in radius is assumed only during the LBM computation phase (fluid and fluid – solid interaction). The reduction in radius allows interconnected pore space through which the surrounding fluid can flow. This technique has no effect on the grain – grain interactions computed using DEM. See Kumar et al. (2012) for more details about the relationship between reduction in radius and permeability of the granular assembly.

For a slope angle of 5°, the hydrodynamic radius of the loosely packed grains was varied from r = 0.7R (high permeability), 0.75R, 0.8R, 0.85R to 0.9R (low permeability). The run-out distance is found to increase with decrease in the permeability of the granular assembly (see Figure 6.14). The run-out distance for high permeable conditions (r = 0.7R – 0.8R) were lower than their dry counterparts. Although, decrease in permeability resulted in an increase in the run-out distance, no significant change in the run-out behaviour was observed for a hydrodynamic radius of up to 0.8R.

With further decrease in permeability (r = 0.85R and 0.9R), the run-out distance in the fluid was greater than the run-out observed in the dry condition. At very low permeability (r = 0.9R), granular material started to entrain more water at the base, which causes a reduction in the effective stress accompanied by a lubrication effect on the flowing granular media. This can be seen as a significant increase in the peak kinetic energy and the duration of the peak energy, in comparison with dry and high permeable conditions (see Figure 6.16).

The permeability of the granular column did not have an influence on the evolution of height during the flow. However, dry granular column tends to collapse more than the immersed granular column (see Figure 6.15).

Positive pore-pressure generation at the base of the flow was observed for low permeable conditions. Inspection of the local packing density showed entrainment of water at the base of the flow, which can also be observed by the steep decrease in the packing density (see Figure 6.17) for the very low permeability condition (r = 0.9R). At the end of the flow ($t \geq 3 \times \tau_c$), the excess pore-pressure dissipates and the granular material, irrespective of their permeability, reaches almost the same packing density.

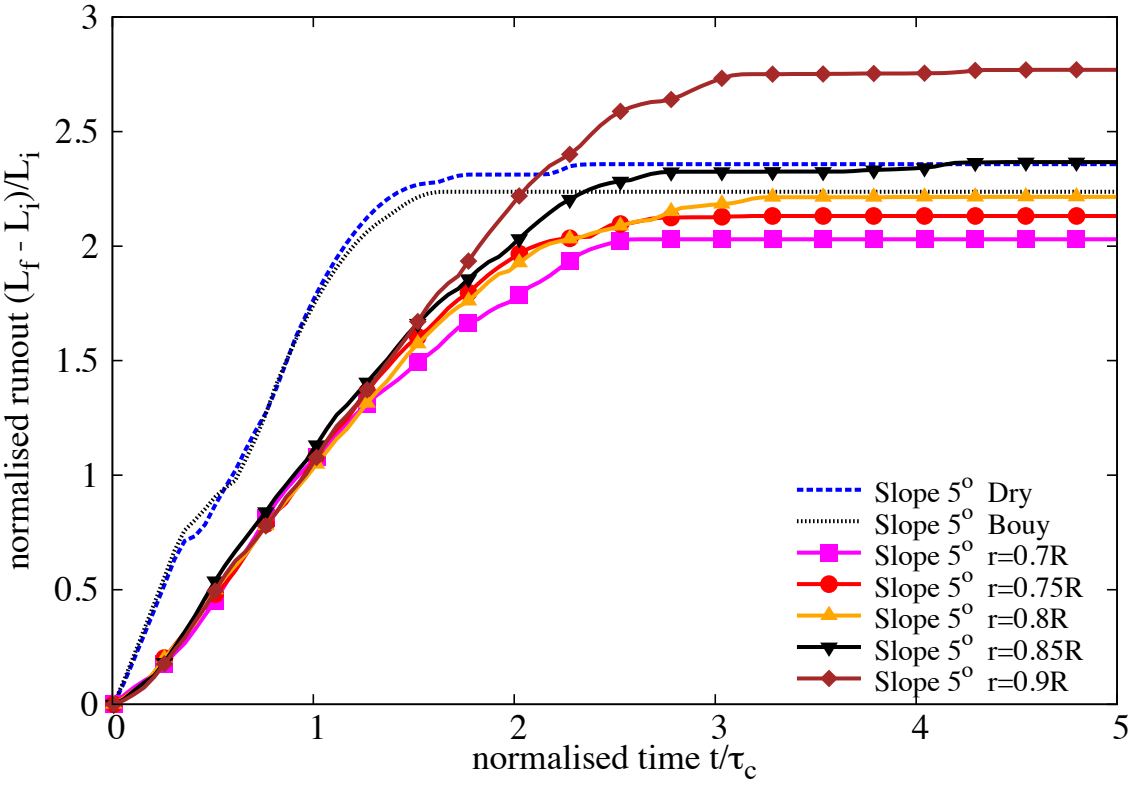


Figure 6.14 Evolution of run-out with time for different permeability (loose slope 5°)

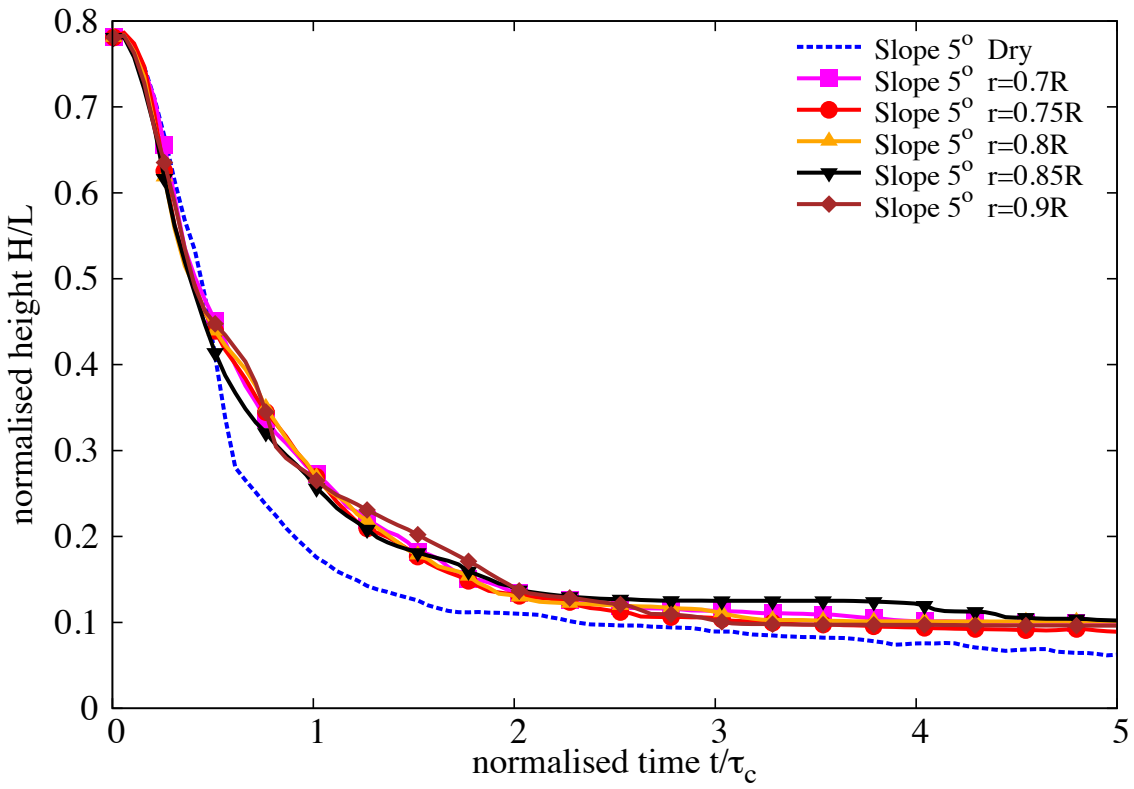


Figure 6.15 Evolution of height with time for different permeability (loose slope 5°)

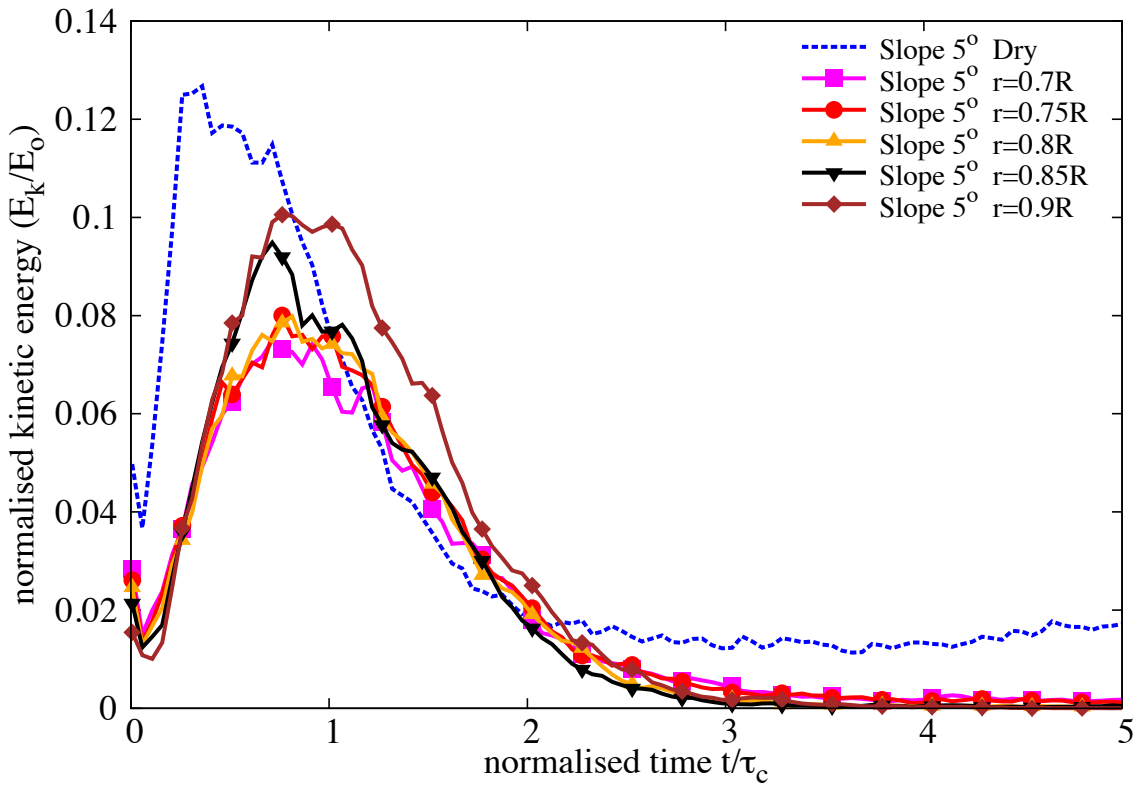


Figure 6.16 Evolution of Kinetic Energy with time for different permeability (loose slope 5°)

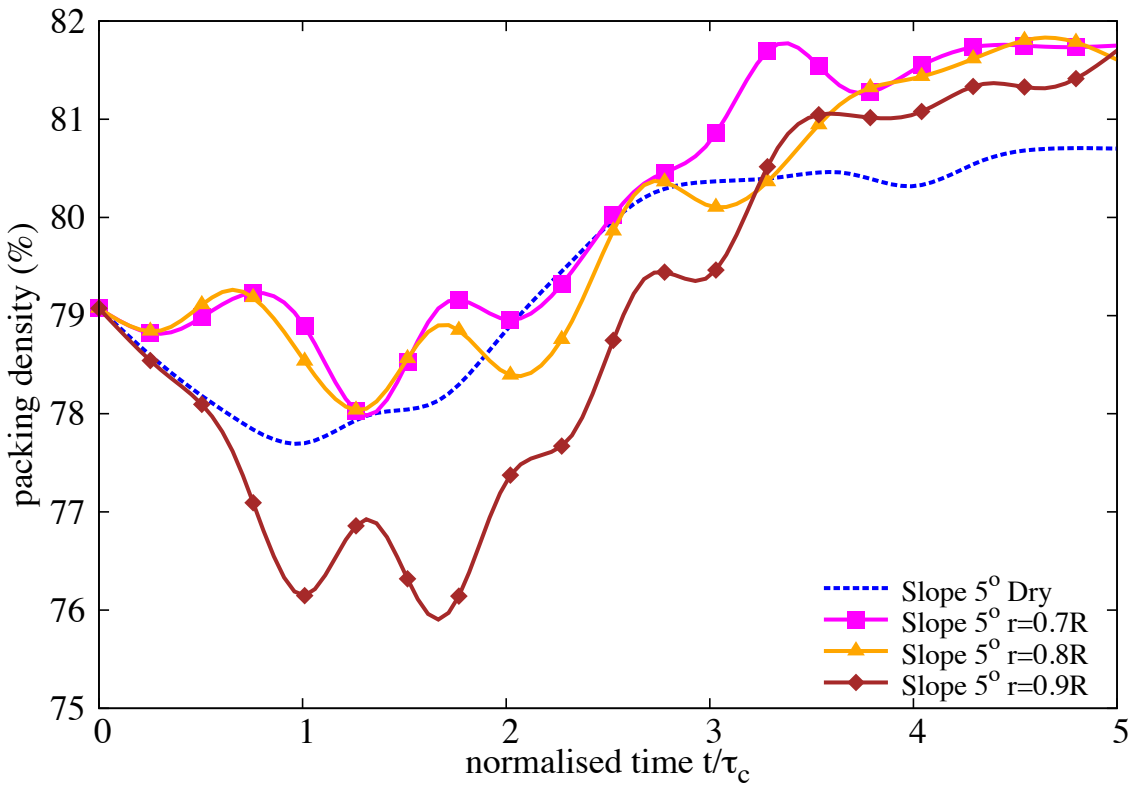


Figure 6.17 Evolution of packing density with time for different permeability (loose slope 5°)

### 6.3.3 Summary

Two-dimensional LB-DEM simulations were performed to understand the behaviour of submarine granular flows. Unlike dry granular collapse, the run-out behaviour in fluid is dictated by the initial volume fraction. Granular columns with loose packing tend to flow longer in comparison to dense columns, due to entrainment of water at the base resulting in lubrication. The loose column when it starts flowing expands and ejects liquid, leading to a partial fluidization of the material. However, with increase in the slope angle, the run-out in fluid is influenced by the viscous drag on the granular materials. The run-out distance in fluid increases with decrease in permeability. More research work is required to characterise the flow behaviour of granular materials, especially in submerged conditions.

# References


Bonnet, F., Richard, T., and Philippe, P. (2010). Sensitivity to solid volume fraction of gravitational instability in a granular medium. *Granular Matter*.

Denlinger, R. and Iverson, R. (2001). Flow of variably fluidized granular masses across three-dimensional terrain, ii: Numerical predictions and experimental tests. *J. Geophys. Res*, 106(B1):553–566.

Iverson, R. M. (2000). Acute Sensitivity of Landslide Rates to Initial Soil Porosity. *Science*, 290(5491):513–516.

Kumar, K., Soga, K., and Delenne, J.-Y. (2012). *Discrete Element Modelling of Particulate Media*. Special Publication. Royal Society of Chemistry, Cambridge.

Mansouri, M., Delenne, J. Y., El Youssoufi, M. S., and Seridi, A. (2009). A 3D DEM-LBM approach for the assessment of the quick condition for sands. *Comptes Rendus Mécanique*, 337(9-10):675–681.

Meruane, C., Tamburrino, A., and Roche, O. (2010). On the role of the ambient fluid on gravitational granular flow dynamics. *Journal of Fluid Mechanics*, 648:381–404.

Midi, G. D. R. (2004). On dense granular flows. *European Physical Journal E*, 14(4):341–365.

Pailha, M., Pouliquen, O., and Nicolas, M. (2008). Initiation of Submarine Granular Avalanches: Role of the Initial Volume Fraction. *AIP Conference Proceedings*, 1027(1):935–937.

Peker, S. and Helvacı, S. (2007). *Solid-liquid two phase flow*. Elsevier.

Rondon, L., Pouliquen, O., and Aussillous, P. (2011). Granular collapse in a fluid: Role of the initial volume fraction. *Physics of Fluids*, 23(7):073301–073301–7.

Thompson, E. L. and Hupper, H. E. (2007). Granular column collapses: Further experimental results. *Journal of Fluid Mechanics*, 575:177–186.

Topin, V., Dubois, F., Monerie, Y., Perales, F., and Wachs, A. (2011). Micro-rheology of dense particulate flows: Application to immersed avalanches. *Journal of Non-Newtonian Fluid Mechanics*, 166(1-2):63–72.

Topin, V., Monerie, Y., Perales, F., and Radjaï, F. (2012). Collapse Dynamics and Runout of Dense Granular Materials in a Fluid. *Physical Review Letters*, 109(18):188001.